

# Centrifuge Modelling of Lateral Spreading Past Pile Foundations

S.K. Haigh & S.P.G. Madabhushi  
*University of Cambridge, UK*

**ABSTRACT:** Lateral spreading past pile foundations has been the cause of foundation failures in several major earthquakes. A series of centrifuge tests have been carried out in order to study the soil-pile interaction taking place. This paper will discuss the observed behaviour, specifically the variation of pore-pressures close to the piles and the bending moments induced in them.

## 1 INTRODUCTION

Lateral spreading of sloping liquefiable deposits has been seen to be one of the most damaging liquefaction-induced effects in earthquakes. According to the National Research Council's report (1985) this has caused more damage than any other form of liquefaction-induced ground failure.

The mechanisms by which lateral spreading can cause damage can be grouped into two major areas:

- Damage due to settlement, e.g. deformation of dams or embankments.
- Damage due to lateral movement of soil past foundations or pipelines.

In this paper, the second mechanism of damage will be discussed with specific reference to lateral spreading past pile foundations.

To illustrate the damage that may be caused to pile foundations by lateral spreading, it is useful to consider an example. One graphic example of this failure mechanism is exhibited by the collapse of the Showa bridge during the 1964 Niigata earthquake. The damage to this bridge is illustrated by figure 1, which shows the collapsed state of the bridge after the earthquake. It can be seen that the decks of the bridge have fallen off the bearings on the piers at one end of them, resulting in the complete collapse of the bridge.



Figure 1. Collapse of the Showa bridge in the 1964 Niigata earthquake (after Hamada 1992).

Analysis by Hamada (1992) illustrates the mechanism of failure. The bridge piers are founded on 25m long 30cm diameter steel pipe piles. These were deflected laterally by approximately 1m at the bridge deck under the action of lateral flow of soil, sufficient to cause the decks to fall off the piers into the river. The failure being the result of lateral spreading rather than inertial effects is confirmed by eye-witness accounts that speak of the collapse occurring a short time after the completion of shaking.

The deformed shape of the pile is illustrated by figure 2.

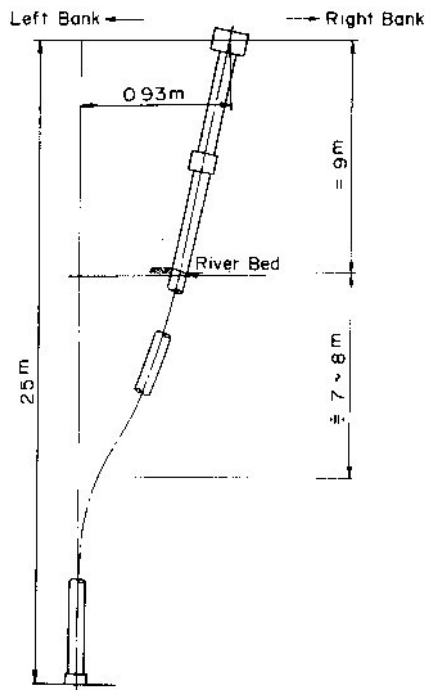


Figure 2. Deformation of the piles of the Showa bridge (after Hamada, 1992).

This paper will discuss the results of a series of centrifuge tests carried out to investigate the interaction between flexible piles and laterally flowing soil. Specific reference will be made to the difference in soil behaviour that is observed immediately upslope and downslope of the pile and the effect that this has on the forces exerted on the pile.

## 2 CENTRIFUGE TESTING

Centrifuge tests were carried out on liquefiable slopes containing flexible model piles, strain-gauged to measure induced bending moments. The model slopes also contained accelerometers (ACC's) to measure the variation of acceleration through the soil layer and pore pressure transducers (PPT's) to monitor liquefaction and the soil behaviour at various locations within the model.

The model geometry and instrument layout for test SKH-14, whose results will be discussed in this paper are shown in figure 3. This model contained two piles whose properties are summarised in table 1. These piles are constructed from an aluminium alloy skeleton, strain-gauged to measure bending moments, encased in high-density closed-cell foam. This allows relatively flexible piles to be constructed without very thin-walled tubes needing to be used. The two piles used had square and circular cross-sections, with the same overall stiffness, this was in order to attempt to quantify any variations in loading that might be encountered due to variation in pile shape. This will not however be discussed in this paper.

Table 1. Properties of model piles (prototype scale)

Property	Value
Length	6.5 m
Diameter	1 m
EI	16.25 MNm <sup>2</sup>
Mp	250 kNm

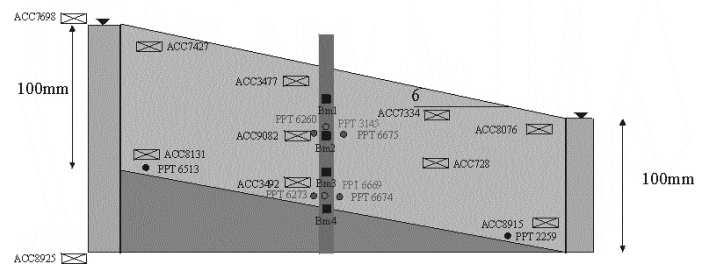


Figure 3. Instrument layout in test SKH-14

These piles are very flexible when compared with true piles of the same diameter. This situation was chosen as failure due to lateral spreading is primarily a problem of small diameter piles, as the applied loading will vary linearly with diameter, whereas the plastic modulus will vary with the diameter cubed. In the centrifuge, however, small piles bring in added problems with both manufacturing and particle-size effects. It was thus decided to make what is in practice a very unlikely pile, in order to gain measureable loading and deformations. Once the loading on these larger diameter piles has been determined, this can be referred back to the behaviour of more realistic piles.

It can be seen that instrumentation is present for measuring the pore-pressures on the front and back faces of the piles, as well as in the free-field. This will allow the stress paths of soil elements close to the pile to be investigated and compared.

### 2.1 Model preparation

The model consists of a wedge shaped layer of dense fraction E silica sand at the base of the box, overlain by a 100mm thick layer of loose, liquefiable fraction E sand. The properties of this sand are summarised in table 2. At the ends of the box are drains formed from coarse fraction B silica sand to give a plane-strain seepage condition.

The model was prepared by air pluviation from an overhead hopper, with the dense layer being formed by pouring slowly and the loose layer by pouring quickly. The dense layer had a relative density of approximately 70%, whereas the loose layer had relative density 40%. The model was poured with the model piles already in-situ, not modelling any installation effects from pile driving or boring. The model was constructed within an Equivalent Shear Beam (ESB) model container whose stiffness is matched to the soil column within it in order to minimise stress wave reflection from the end walls.

This container is described in detail by Zeng & Schofield (1996).

Table 2. Properties of fraction E silica sand

Property	Value
$D_{10}$ grain size	0.095 mm
$D_{50}$ grain size	0.14 mm
$D_{90}$ grain size	0.15 mm
Specific gravity $G_s$	2.65
Minimum voids ratio $e_{min}$	0.613
Maximum voids ratio $e_{max}$	1.014
Permeability at $e=0.72$	$0.98e-4 \text{ ms}^{-1}$
Critical state friction angle $\phi_{crit}$	$32^\circ$

The model was then saturated from the base under vacuum with 50 centiStoke silicone oil in order to correct the centrifuge scaling laws for velocity. Once saturated, the model was loaded onto the Cambridge Stored Angular Momentum (SAM) actuator, whose design and performance are described by Madabhushi et al (1998), and then loaded onto the Cambridge 10m beam centrifuge.

## 2.2 Model Testing

Once at 50g, steady state seepage was achieved by pumping silicone oil into the reservoir at the top of the slope by means of a peristaltic pump. Overflows were present at the surface of the top and bottom reservoirs in order to keep the water-table at the surface here, with the waste oil being recirculated. Once steady-state seepage was observed from the PPT records, (after a period of approximately 2 hours), an earthquake of magnitude 25%g, duration 0.9 s and frequency 50 Hz was fired. This corresponds to a 25% earthquake of 1 Hz fundamental frequency and 45 second duration at prototype scale.

Data was logged using the CDAQS system that features on-board digitisation of data, which is then downloaded via a serial link.

Further details of the experimental setup and procedures can be found in Haigh et al. (2000).

## 3 TEST RESULTS AND ANALYSIS

The results from this experiment will be discussed in three parts, the behaviour of the free-field slope, induced bending moments in the pile and behaviour of the soil close to the pile.

### 3.1 Free-field behaviour

As can be seen from figure 4 which shows the generation of excess pore pressures measured for the column of instruments in the free field, full liquefaction of the soil bed was observed with around 10kPa of cycling of pore pressures during the earthquake.

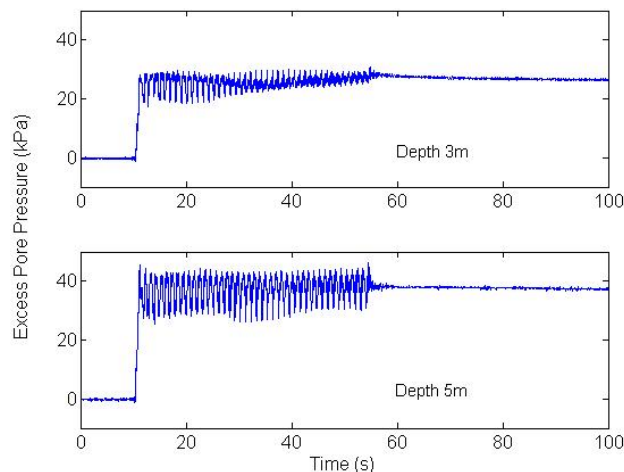


Figure 4. Free-field excess pore pressure time-histories

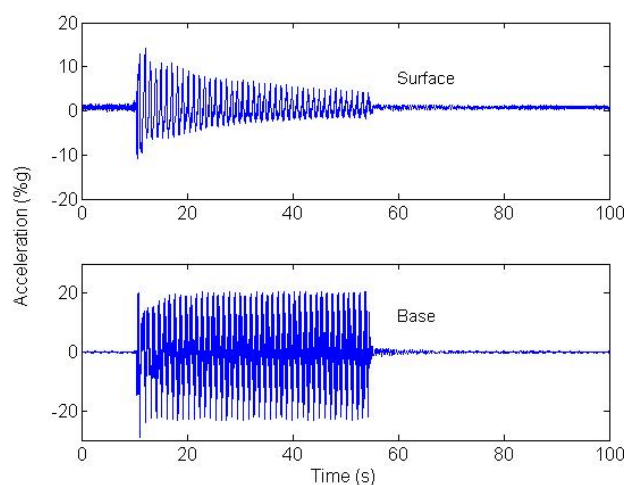


Figure 5: Accelerations measured at base and surface of model.

Due to the looseness of the soil and the relatively high lateral accelerations experienced by the soil, initial liquefaction occurs in approximately one cycle.

Figure 5 shows the accelerations measured at the base and surface of the model. The accelerations measured at the surface of the model can be seen to have been attenuated and to have become significantly asymmetric owing to the slope of the model surface. Negative (upslope) accelerations are truncated due to sliding occurring within the model, whereas the greater shear stresses required to cause upslope sliding to occur give less attenuation of the positive accelerations.

### 3.2 Induced bending moments

The two piles present in the model were each instrumented with four strain-gauged bridges in order to measure the induced bending moments.

Time histories of bending moments at three of the bridges in one pile are shown in figure 6,

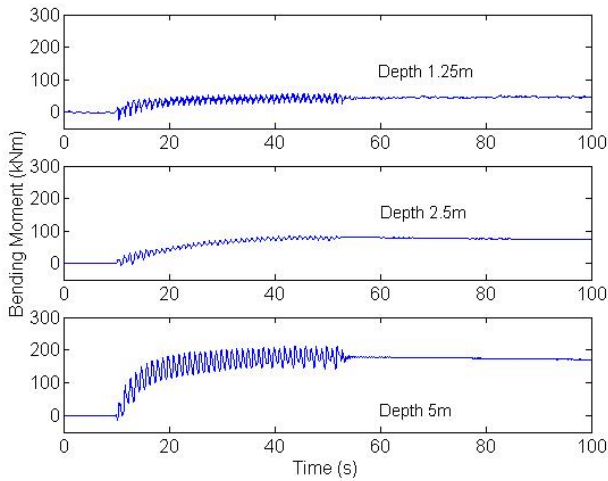


Figure 6. Bending moment time-histories

unfortunately the fourth gauge malfunctioned and gave no data.

It can be seen that base bending moments of approximately 200kNm are induced in the pile. These appear to vary almost linearly with depth, suggesting that the predominant lateral loading is coming from a non-liquefied surface layer which would be present due to g-field curvature. This layer is approximately 0.75m thick, passive pressure from which would contribute 40% of the measured base-moments. The rest of the moments are contributed by lateral pressures from the flow of the liquefied soil.

It can be seen from study of the bending moment measured at 5m depth that the bending moment picks up a significant harmonic at 0.5 Hz towards the end of the earthquake. This is also present in the surface acceleration measured close to the pile and is a feature of resonance of the liquefied soil column.

It was seen that the bending moments induced in the square piles were approximately 5% greater than those in the circular pile, similar to the theoretical value of approximately 7% which can be obtained from considering upper and lower bound mechanisms for laterally loaded piles in cohesive materials.

### 3.3 Near-pile soil behaviour

The soil behaviour close to the pile was observed by means of pairs of PPT's placed around 10mm from the pile surface both upslope and downslope of the pile. A typical set of results from these is shown in figure 7, showing the upslope, free-field and downslope pore-pressures recorded at 3m depth (prototype scale).

It can be seen that close to the pile, the amount of cycling observed in the excess pore-pressures is much greater than that observed in the free-field. It can also be seen that downslope of the pile, very

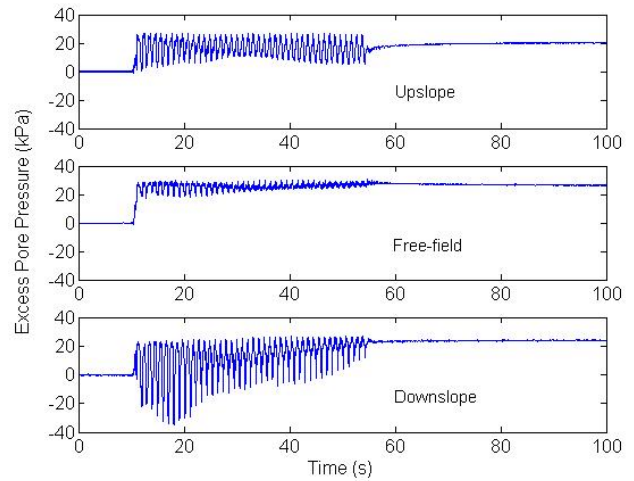


Figure 7. Pore-pressures measured near pile at 3m depth

large cyclic behaviour is observed, with pore-pressures being in suction, relative to the hydrostatic condition. This behaviour can be explained with reference to the stress-paths occurring at the soil elements using characteristic state theory, as proposed by Luong & Sidaner (1981). This is shown in figure 8, which illustrates the drained and undrained stress paths for elements immediately upslope and downslope of the pile.

Characteristic state theory proposes that dilative and contractile regions in  $q$ - $p'$  space are separated by two straight lines, termed the characteristic state lines, at which soil elements will shear at constant volume in the drained condition. Soil elements between these lines will tend to contract (or generate positive pore-pressures) when sheared, whereas soil elements outside these lines will show dilative behaviour.

Upslope of the pile, horizontal stresses are increased with soil flow, resulting in a drop in deviatoric stress, whereas downslope of the pile, horizontal stresses are relaxed, resulting in an increase in deviatoric stress. It can be seen from figure 8 that because in the initial condition the coefficient of earth-pressure  $K$  is less than unity, the initial

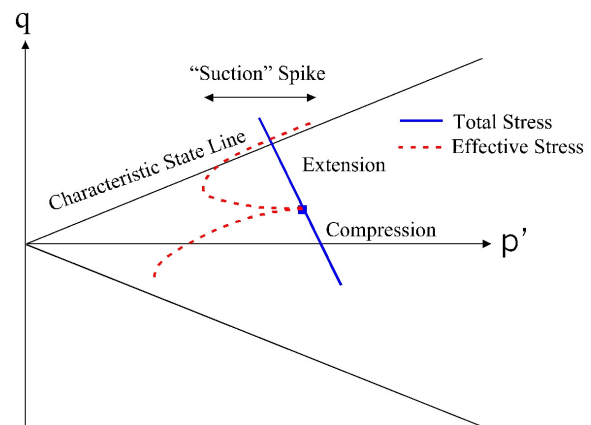


Figure 8. Stress paths of elements in front of and behind the pile.

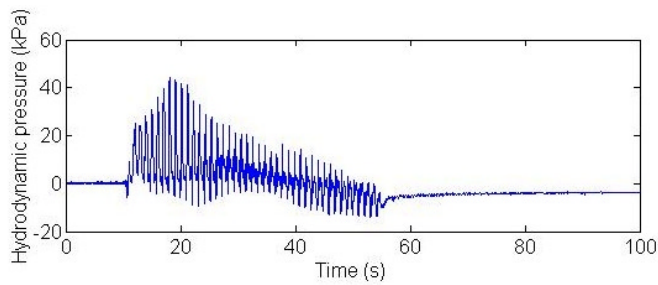


Figure 9. Net downslope hydrodynamic force acting on pile

deviatoric stress causes the stress path for the soil downslope of the pile to reach the characteristic state line and to begin dilating before the soil element upslope of the pile. Thus more dilative behaviour is seen downslope of the pile than upslope.

This behaviour causes a net downslope hydrodynamic force to act on the pile, a time-history of which is shown in figure 9, obtained from the difference between measured pore-pressures upslope and downslope of the pile.

It can be seen that the peak value of this hydrodynamic pressure is approximately 45 kPa, a significant loading when one considers that the vertical effective stress at this depth is approximately 30 kPa.

The Japanese highway bridges (Japan Road Association 1996) design code states that when designing piles for lateral flow of liquefied soil, one should design for a horizontal pressure of 30% of overburden stress. This would amount to a pressure of 18 kPa in this case, significantly less than the pore-pressure difference between the faces of the pile, measured in this experiment, regardless of any horizontal effective stress difference that might also contribute to the loading.

If we assume that this 45kPa lateral loading is a triangular loading with depth, this would predict base bending moments of approximately 270 kPa, significantly higher than those measured and discussed in section 3.2, even discounting contributions from the non-liquefied crust. One method of reconciling this anomaly is by virtue of the dynamic response of the pile. Bending moments are a feature of displacement rather than directly being a feature of loading, being the local curvature multiplied by the stiffness of the pile. Under pseudo-static conditions, this distinction is not important as the body remains approximately in equilibrium at all times. However, for dynamic and transient loading in which significant body accelerations are occurring, equilibrium is not satisfied. Thus the relationship between loading frequency and the natural frequency of the body being considered is important when relating applied forces to induced displacements (or bending moments).

This is illustrated by figure 10 which shows the response of a first-order linear system to harmonic excitation. The y-axis shows the amplification of displacement over that which would be expected for a static load and the x-axis shows the ratio of the forcing frequency to the natural frequency of the system.

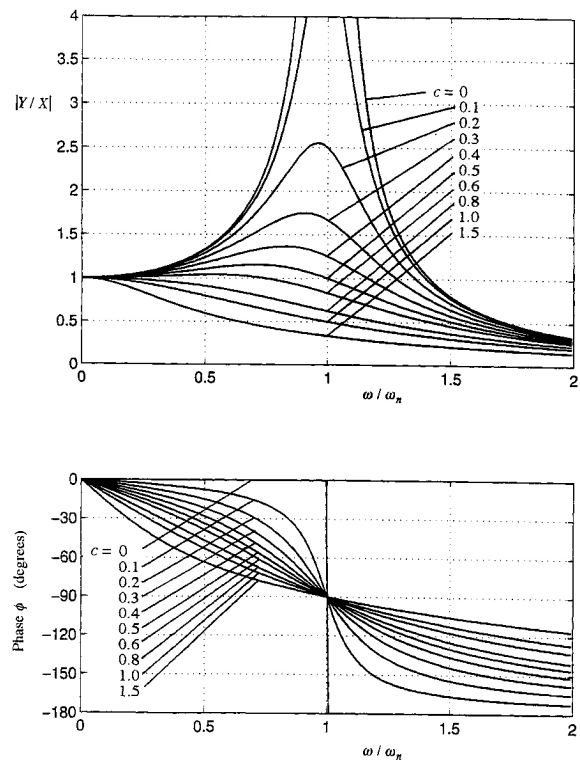


Figure 10. Response of a linear first-order system. (CUED 2000)

It can be seen that if the pile has significant damping and/or is being excited at a frequency significantly higher than its natural frequency, the resultant displacements and hence bending moments will be less than might be predicted by consideration of the forces acting on the body.

#### 4 CONCLUSIONS

The lateral loading of piles by laterally-spreading liquefied soil was investigated by centrifuge modelling. It was shown that while much of the loading can be accounted for by a non-liquefied crust, significant loading is also applied by the flowing liquefied soil.

Measurement of pore-pressures close to the upslope and downslope surfaces of the pile was instrumental in revealing the soil behaviour taking place. Significant dilation was observed near the downslope surface of the pile, causing pore-pressure differences of up to 45 kPa between the pile faces.

Dynamic response of the pile is important in determining whether or not these transient forces are

attenuated when experienced by the pile in terms of bending moments.

## ACKNOWLEDGEMENTS

The authors would like to thank the Engineering and Physical Sciences Research council who funded this research.

## REFERENCES

- CUED, 2000. *Mechanics Databook*, Cambridge, UK: Cambridge University Engineering Department.
- Haigh, S.K., Madabhushi, S.P.G., Soga, K., Taji, Y. & Shamoto, Y. 2000. Lateral spreading during centrifuge model earthquakes, *Proc. GeoEng2000, Melbourne, November 2000*
- Hamada, M. 1992. Large ground deformations and their effects on lifelines: 1964 Niigata earthquake, In Hamada & O'Rourke (eds.), *Case studies of liquefaction and lifeline performance during past earthquakes*, Technical report NCEER-92-0001. Buffalo, NY:NCEER.
- Japan Road Association 1996. *Specifications for highway bridges, Part V: Seismic Design*, (in Japanese)
- Luong, M.P. & Sidaner, J.F. 1981. Undrained behaviour of cohesionless soils under cyclic and transient loading, In Prakash (ed.), *Proc. Int. Conf. Recent Advances in Geotechnical Earthquake Engineering and Soil Dynamics, St Louis, 26 April - 3 May 1981*. Rolla, MO: University of Missouri-Rolla
- Madabhushi, S.P.G., Schofield, A.N. & Lesley, S. 1998. A new stored angular momentum (SAM) based earthquake actuator. In Kimura, Kusakabe & Takemura (eds.), *Proc. Int. Conf. Centrifuge '98, Tokyo, 23-25 September 1998*. Rotterdam: Balkema.
- National Research Council 1985. *Liquefaction of soils during earthquakes*. Washington, DC: National Academy Press.
- Zeng, X. & Schofield, A.N. 1996. Design and performance of an equivalent shear beam container for earthquake centrifuge modelling, *Géotechnique* 46(1):83-102